letters to nature

23. Gray, W. M., Kepinski, S., Rouse, D., Leyser, O. & Estelle, M. Auxin regulates SCF^TIR1-dependent degradation of AUX/IAA proteins. *Nature* **414**, 271–276 (2001).
24. Connelly, C. & Hieter, P. Budding yeast *SKP1* encodes an evolutionarily conserved kinetochore protein required for cell cycle progression. *Cell* **86**, 275–285 (1996).
25. Tzfira, T., Vaidya, M. & Citovsky, V. Increasing plant susceptibility to *Agrobacterium* infection by overexpression of the *Arabidopsis VIP1* gene. *Proc. Natl Acad. Sci. USA* **99**, 10435–10440 (2002).
26. Lee, D. H. & Goldberg, A. L. Proteasome inhibitors: valuable new tools for cell biologists. *Trends Cell Biol.* **8**, 397–403 (1998).
27. Narasimhulu, S. B., Deng, X.-B., Sarria, R. & Gelvin, S. B. Early transcription of *Agrobacterium* T-DNA genes in tobacco and maize. *Plant Cell* **8**, 873–886 (1996).
28. Otten, L. *et al.* Restoration of virulence of *vir* region mutants of *A. tumefaciens* strain B6S3 by coinfection with normal and mutant *Agrobacterium* strains. *Mol. Gen. Genet.* **195**, 159–163 (1984).
29. Schrammeijer, B., Hemelaar, J. & Hooykaas, P. J. The presence and characterization of a *virF* gene on *Agrobacterium vitis* Ti plasmids. *Mol. Plant Microbe Interact.* **11**, 429–433 (1998).
30. Nagai, H. & Roy, C. R. Show me the substrates: modulation of host cell function by type IV secretion systems. *Cell. Microbiol.* **5**, 373–383 (2003).

....

Centrosomes direct cell polarity independently of microtubule assembly in *C. elegans* embryos

Carrie R. Cowan & Anthony A. Hyman

Max Planck Institute of Molecular Cell Biology and Genetics, Pfotenhauerstrasse 108, Dresden 01307, Germany

....

Polarity establishment requires a symmetry-breaking event, resulting in an axis along which determinants are segregated. In *Caenorhabditis elegans*, oocytes are apolar and are triggered to polarize rapidly along one axis after fertilization. The establishment of this first polarity axis is revealed by the asymmetric distribution of PAR proteins and cortical activity in the one-celled embryo. Current evidence suggests that the centrosome–pronucleus complex contributed by the sperm is involved in defining the polarization axis[1–6]. Here we directly assess the contribution of the centrosome to polarity establishment by laser ablating the centrosome before and during polarization. We find that the centrosome is required to initiate polarity but not to maintain it. Initiation of polarity coincides with the proximity of the centrosome to the cortex and the assembly of pericentriolar material on the immature sperm centrosome. Depletion of microtubules or the microtubule nucleator γ-tubulin did not affect polarity establishment. These results demonstrate that the centrosome provides an initiating signal that polarizes *C. elegans* embryos and indicate that this signalling event might be independent of the role of the centrosome as a microtubule nucleator.

After fertilization, the PAR proteins are uniformly distributed in the *C. elegans* embryo[5,7–9]. Coincident with the completion of female meiosis, about 30 min after fertilization, shallow ingressions ('ruffles') become visible throughout the cortex. On perception of a polarization signal a few minutes later, the PAR proteins segregate

into their anterior (PAR-3 and PAR-6)[5,8,9] and posterior (PAR-1 and PAR-2)[5,7,10] domains. Concomitantly, contractile polarity is established[5]: the anterior cortex continues to ruffle while cortical activity in the posterior ceases, creating a smooth domain. The male pronucleus and microtubule asters lie adjacent to the smooth, posterior PAR-2 domain[5,6]. To investigate when centrosome–cortex proximity occurs relative to the initiation of polarity, centrosome position was monitored with a green fluorescent protein (GFP)-tagged centrosome marker, SPD-2 (ref. 11), and polarity was assessed both by GFP–PAR-2 (Fig. 1a; Supplementary Movie 1) and by cortical ruffling. The initiation of cortical polarity was evident as a progressive cessation of ruffling, spreading from a focus on the cortex, and within 2 min GFP–PAR-2 was visible on the expanding smooth cortex. Before the onset of polarization, the centrosome–cortex distances were variable (Fig. 1b; the range at −3:20 (3 min 20 s before the onset of posterior smoothing) was 0–9 μm; n = 9). However, we consistently observed that the centrosome was closest to the cortex when cortical polarity was initiated (Fig. 1b; range at 0:00 was 0–4 μm; n = 14). Thus, polarity initiation coincided with centrosome–cortex proximity.

As a direct test of the role of the centrosome in polarity establishment, centrosomes were located during female meiosis with the use of GFP–SPD-2 fluorescence and the labelled centrosomes were ablated with a pulsed ultraviolet-laser microbeam. Polarity was assessed by time-lapse imaging of GFP–PAR-2 or contractile polarity. Successful ablations were judged by the absence of a GFP–SPD-2 structure throughout the recording period (minimally 30 min after ablation) and a failure of the fast phase of pronuclear migration, a phenotype associated with centrosome defects. In embryos in which the centrosome was successfully ablated before the onset of polarity, no asymmetric PAR-2 localization was observed (n = 30; Fig. 2a; Supplementary Movies 2 and 3) and ruffling continued throughout the entire cortex (Supplementary
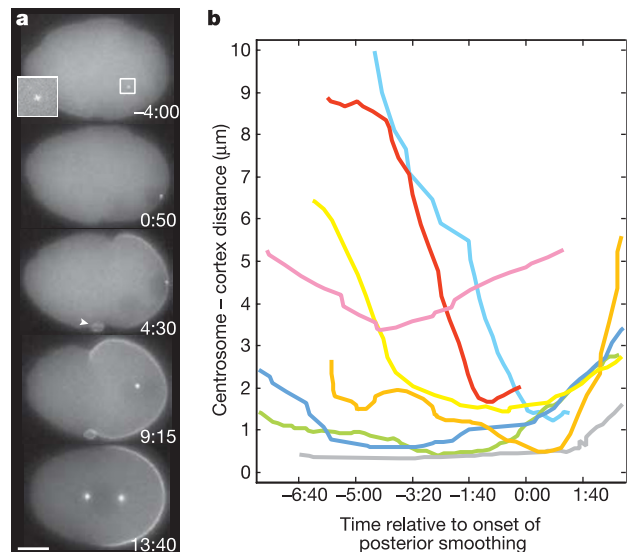

Figure 1 The centrosome lies adjacent to the cortex at the time of polarity initiation. **a**, Time lapse images of a GFP–PAR-2; GFP–SPD-2 embryo (Supplementary Movie 1). The GFP–SPD-2-labelled centrosome is visible as a bright cytoplasmic dot (the second centrosome is out of the focal plane); GFP–PAR-2 labels the posterior cortex. The small ring of GFP–PAR-2 (arrowhead, 4:30) corresponds to the polar body cortex. The embryo posterior is to the right. Scale bar, 10 μm. **b**, Centrosome–cortex distances during polarity establishment. Solid lines indicate the distance (μm) from the centrosome to the nearest point on the cortex over time. PAR-2 polarity was established at about 2:00 (see Methods). Times were standardized to the onset of posterior smoothing, indicating polarity establishment. Only a subset of experiments is shown.

Movie 2). In the experiments in which GFP–SPD-2 reappeared after less than 5 min, indicating that the centrosome had probably been photobleached rather than destroyed, normal PAR-2 polarity was established. Similarly, if the nucleus or cytoplasm in the vicinity of the centrosome, or a cortical region away from the centrosome, was

Figure 2 Centrosome ablation prevents polarity establishment but not the propagation and maintenance of the posterior domain. **a**–**c**, Time-lapse images of GFP–PAR-2 polarity after centrosome ablation. The first frame ('pre-ablation') in each series immediately precedes the ablation; the time elapsed after centrosome ablation is indicated in minutes:seconds. The embryo posterior is to the right. Scale bars, 10 μm. **a**, Centrosome ablation before polarity establishment (Supplementary Movies 2 and 3). Embryos in which the centrosomes were not adjacent to the cortex were chosen for ablation, to eliminate the possibility of damaging the cortex. Either one or two closely spaced GFP–SPD-2 dots were visible. **b**, Centrosome ablation during polarity establishment (Supplementary Movie 5). Ablations were performed on embryos in which the centrosomes (two closely spaced GFP–SPD-2 dots) were near the cortex and the posterior domain (judged by ruffling and GFP–PAR-2) occupied less than half the embryo length. Arrows indicate the boundaries of the 'pre-ablation' posterior domain; GFP–PAR-2 is present only weakly although ruffling has ceased. In **a** and **b** the small ring of GFP–PAR-2 at the anterior (arrowhead) corresponds to the polar body cortex. **c**, Centrosome ablation after polarity establishment (Supplementary Movie 6). Polarity was considered to be established when the posterior domain occupied half the embryo length. The centrosomes had moved away from the cortex and separated around the nuclear envelope. The two centrosomes were ablated individually. **d**, Relation between pre-ablation and post-ablation PAR-2 domain extension. Bars represent the percentage of the anterior–posterior axis of the embryo occupied by cortical PAR-2. Control ablations represent embryos in which the cortex rather than the centrosome was ablated (Supplementary Movie 7). Only a subset of experiments is shown.

ablated, asymmetric PAR-2 localization occurred normally ($n = 19$; Supplementary Movie 4), indicating that only centrosome ablation inhibits the establishment of polarity. We conclude that the centrosome, or a closely associated cellular component, is required to establish polarity in the one-cell *C. elegans* embryo.

The centrosome could be required continuously during polarity establishment or could provide a transient symmetry-breaking signal. To distinguish between these ideas, we laser ablated the centrosome at different times during polarity establishment. If embryos had initiated but not yet completed polarization, the GFP–PAR-2 domain expanded in the absence of the centrosome (Fig. 2b; Supplementary Movie 5). If the centrosome was ablated after polarity establishment, polarity was maintained (Fig. 2c; Supplementary Movie 6). We therefore conclude that the centrosome is required to initiate polarity but not to propagate or maintain it.

Although polarity maintenance occurred in the absence of centrosomes, the PAR-2 domain was smaller than in control embryos. In control ablation embryos, PAR-2 expanded to $53 \pm 10\%$ egg length ($n = 8$). If the centrosomes were ablated in the early stages of PAR-2 spreading, PAR-2 expanded to only $37 \pm 7\%$ egg length ($n = 14$). If the centrosomes were ablated after the domain had formed (PAR-2 extended to about 50% of egg length), PAR-2 seemed to regress ($n = 5$). All embryos showed a narrow range of final GFP–PAR-2 extension after centrosome ablation (Fig. 2d, black dots), despite having various sizes of initial posterior domains (Fig. 2d, grey bars). We therefore conclude that expansion of the PAR-2 domain is largely independent of the centrosome but that full extension of the domain requires a centrosome-dependent process. Taken together, our experiments indicate that the centrosomes might provide a transient signal that determines the polarity of the *C. elegans* embryo, but propagation of this polarity can occur without centrosomes.

The centrosome contributed by the sperm is immature and is therefore incapable of microtubule nucleation. About 30 min after fertilization, the centrosome accumulates pericentriolar material[12] (PCM) and initiates microtubule nucleation[13]. To relate the state of centrosome assembly to the onset of polarity, we tracked the fluorescence intensity of GFP-labelled SPD-5, a centrosomal protein that is required for the accumulation of the known PCM components[1]. SPD-5 appeared on the centrosome roughly simultaneously with polarity initiation (Fig. 3a, red line). At about the same time, the microtubule nucleator γ-tubulin[12,14] accumulated on the centrosome (Fig. 3a, blue line). We therefore conclude that polarity initiation occurs concomitantly with the assembly of the PCM at the centrosome.

To investigate the role of PCM assembly in polarity establishment, we first analysed the role of SPD-5, which was previously implicated in PAR protein polarity[1]. We tracked the formation of the GFP–PAR-2 domain over time (Fig. 3b–f) and plotted the boundary (solid green lines) and domain extent (dotted green lines) of cortical PAR-2 and the movement of the pronuclei (blue dots). In control embryos, cortical PAR-2 spread from the posterior pole to the embryo middle during a period of roughly 7 min ($n = 44$; Fig. 3b). In embryos depleted of SPD-5 by RNA-mediated interference (*spd-5(RNAi)*), GFP–PAR-2 was found only in the cytoplasm ($n = 15$; Fig. 3c) and ruffling occurred throughout the entire embryo cortex (Supplementary Fig. 1C) during an equivalent time interval. Similar results were obtained after depletion of SPD-2 ($n = 27$; Fig. 3d; Supplementary Fig. 1D), a protein required for the recruitment of SPD-5 to the centrosome[1,11,15], as shown previously[2]. Thus we conclude that the depletion of PCM components results in the same polarity phenotype as centrosome ablation, which is consistent with previous data[1,2]. We tracked the proximity of the centrosome to the cortex in *spd-5(RNAi)* and *spd-2(RNAi)* embryos and found that centrosome–cortex distances were within the range of control embryos (Supplementary Fig. 2), indicating that both
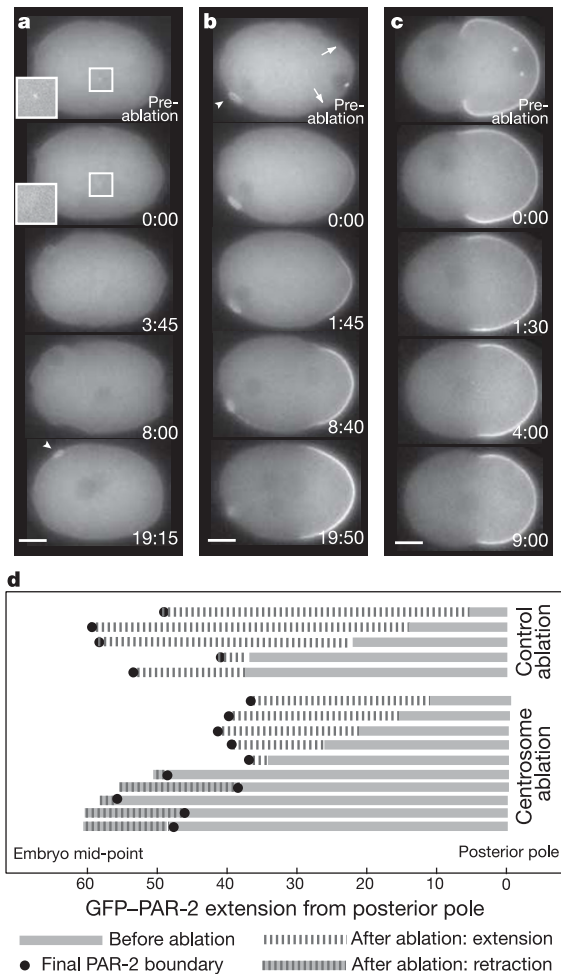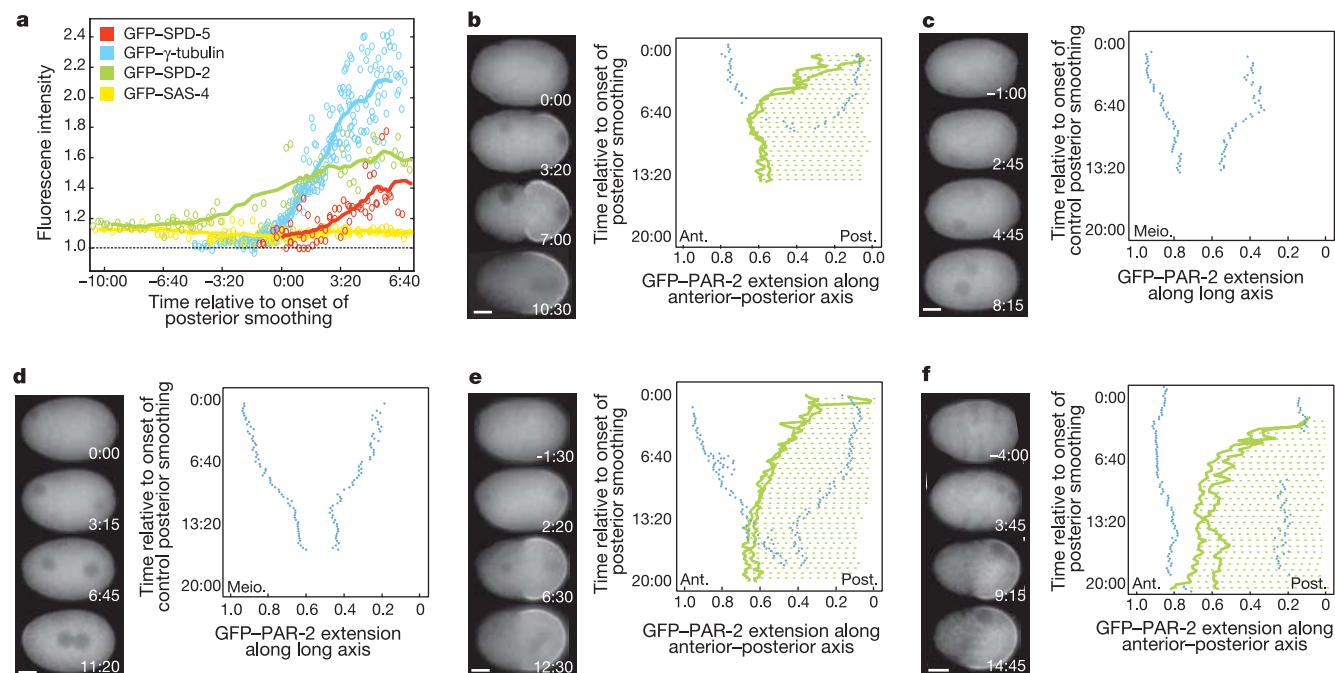
Figure 3 Polarity initiation requires a concomitant assembly of the pericentriolar material. **a**, Kinetics of centrosome assembly relative to polarity establishment. Centrosomal fluorescence is represented as the ratio of cytoplasmic background (1.0 represents no signal). SAS-4, a sperm-provided centriole protein, is shown for comparison. The data represent a minimum of five embryos per centrosome marker. **b**–**f**, Time-lapse images and kymographs (see Methods) of GFP–PAR-2 polarity in control (**b**), *spd-5(RNAi)* (**c**), *spd-2(RNAi)* (**d**), γ-*tubulin(RNAi)* (**e**) and α-/β-*tubulin(RNAi)* (**f**) embryos (similar results were obtained for nocodazole treatment and β-tubulin(RNAi)/ nocodazole; Supplementary Fig. 4). Solid green lines, PAR-2 boundaries; dotted green lines, cortical PAR-2; blue dots, pronuclei. Embryo posterior is to the right. Anterior (ant.) and posterior (post.), or the meiotic pole (meio.) in cases where polarity was not established, are indicated on the graphs; all extensions are shown as fractions of the embryo length. Scale bars, 10 μm. In **a**, **b**, **e** and **f**, times are standardized to the onset of posterior smoothing; in **c** and **d**, times were assigned on the basis of a similar cell cycle stage to that in control embryos at the time of polarization, judged by the size of the male pronucleus and the time elapsed relative to meiosis II. Although *spd-5(RNAi)* and *spd-2(RNAi)* embryos showed no asymmetric PAR-2 distribution during the period of control polarity establishment, some embryos developed small polar patches of PAR-2 at later times (*spd-5(RNAi)*, 11:30 ± 3:40 (*n* = 10); *spd-2(RNAi)*, 11:00 ± 2:20 (*n* = 4)), which is consistent with the polarity defects described for both *spd-5* and *spd-2* mutants[1,2].

SPD-2 and SPD-5 might be required for the polarizing signal.

The depletion of centrosome components thought to be required directly for efficient microtubule nucleation did not affect polarity. Normal polarity was established after the depletion of γ-tubulin (*n* = 36; Fig. 3e; Supplementary Fig. 1E), although no centrosomal microtubules were visible at the time of polarity initiation[12] (Fig. 4a; Supplementary Fig. 3). Similar results were seen after the depletion of other components of the γ-tubulin complex[12] (data not shown). Conversely, the centrosome in *spd-2(RNAi)* embryos nucleated wild-type levels of microtubules at the time of polarity initiation (Fig. 4a; Supplementary Fig. 3), but polarity was not established (Fig. 3d; Supplementary Fig. 1D). There is therefore no obvious correlation between centrosomal microtubule nucleation and polarity establishment.

To further assess the role of microtubules in polarity establishment, we depleted microtubules by using α-/β-*tubulin(RNAi)*, treatment with nocodazole, or a combination of β-*tubulin(RNAi)*/ nocodazole treatment. Microtubule depletion had no effect on the asymmetric localization of GFP–PAR-2 (*n* = 27; Figs 3f and 4) or the polarization of ruffling activity (Supplementary Fig. 1F; Supplementary Fig. 4). Thus polarity establishment in *C. elegans* can occur without a detectable population of microtubules (*n* = 3; Fig. 4b). It seems that the centrosome performs separable functions in the early *C. elegans* embryo, namely microtubule nucleation and polarity establishment.

Previous work indicated that microtubules were sufficient to establish a PAR-2 domain in *C. elegans* embryos during meiosis. Meiosis-arrested embryos exhibited a small cortical PAR-2 patch overlying the meiotic spindle, and formation of this domain was partly inhibited by microtubule depolymerization. This meiotic PAR-2 domain appears transiently in wild-type embryos and seems to form the polar body cortex (Figs 1 and 2). We have found that neither SPD-2 nor SPD-5 is required for the formation of the meiotic PAR-2 domain (C.R.C. and A.A.H., unpublished observations), whereas both are required for embryonic polarity establishment[1,2] (Fig. 3; Supplementary Fig. 1). The mechanisms by which PAR-2 is spatially directed to the cortex therefore differ during meiosis and the subsequent establishment of polarity, perhaps reflecting differences in the underlying mechanisms by which the cortical domains are formed.

On the basis of our experiments, we propose that the centrosome becomes positioned near the embryo cortex simultaneously with the assembly of the PCM about 30 min after fertilization. A signal from the centrosome, which is independent of microtubules, activates a local change in the cortex that, once initiated, propagates independently of the centrosome. The physical change induced in the cortex would result in the cessation of ruffling and allow PAR-2 to localize. Our experiments suggest that both SPD-5 and SPD-2 are required directly for the polarity signal produced by the centrosome.

The proposed centrosome signalling event in the *C. elegans* embryo is reminiscent of microtubule-independent centrosome-mediated reorganization of the cell cortex during blastoderm cellularization in *Drosophila*[16], asymmetric division of *Drosophila* neuroblast precursors[17], and cytokinesis completion in some tissue culture cells[18]. Centrosome-mediated cortical changes are therefore
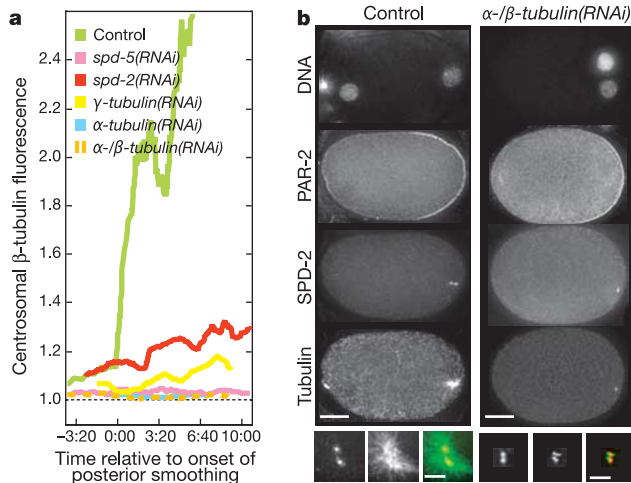
Figure 4 Polarity establishment and microtubule assembly are separable centrosomal functions. **a**, Centrosomal GFP–β-tubulin accumulation after depletion of SPD-5, SPD-2, γ-tubulin, α-tubulin and α-/β-tubulin. Fluorescence intensity is represented as the ratio of cytoplasmic background (1.0 represents no signal). Times are standardized to the onset of posterior smoothing, except for *spd-5(RNAi)* and *spd-2(RNAi)* embryos, for which times were assigned on the basis of a similar cell cycle stage to that in control embryos at the time of polarization, judged by the size of the male pronucleus and the time elapsed relative to meiosis II. The data represent at least five embryos per RNAi condition. **b**, Microtubules and PAR-2 polarity in control and *α-/β-tubulin(RNAi)* embryos. Tubulin images are projections of deconvolved *z*-sections representing the entire cell; PAR-2 and DNA images are projections comprising about one-third of the cell; SPD-2 images are projections encompassing the centrosomal signals. The embryo posterior is to the right. Scale bars, 10 μm. Magnifications correspond to the centrosomal region: left, SPD-2; middle, tubulin; right, merge (red, SPD-2; green, tubulin). Scale bars, 2.5 μm.

likely to occur in many cellular contexts, indicating that they might share an evolutionarily conserved mechanism. □

Methods

Worm strains and time-lapse imaging

All worm strains were maintained at 16 °C and shifted to 25 °C for 20–30 h before recording. Recording of control and RNAi embryos was performed at 20–23 °C; all ablations were performed at 18–20 °C. Embryos were dissected and mounted[19] in a solution containing 0.1 M NaCl and 4% sucrose, with or without 2% agarose. For PAR-2 and centrosomal marker imaging, wide-field GFP and differential interference contrast (DIC) movies were recorded at 15-s intervals, as described previously[20]; GFP–β-tubulin movies were acquired with the use of spinning-disk confocal imaging at 10-s intervals, as described previously[20]. The following strains were used: N2 (wild type), AZ244 (GFP–β-tubulin)[21], JH1380 (GFP–PAR-2)[6], TH26 (GFP–SAS-4)[22], TH27 (GFP–γ-tubulin)[12], TH40 (GFP–SPD-5), TH42 (GFP–SPD-2)[11] and TH49 (GFP–PAR-2; GFP–SPD-2). Amino-terminal GFP-tagged SPD-5 is expressed under the *pie-1* promoter, and transgenic worms were created by microparticle bombardment, as described previously[21].

Data analysis

Data analysis was performed with Matlab (The Math Works, Inc.) and Metamorph (Universal Imaging). Results are given as means ± standard deviations.

Centrosome–cortex distances

Distances were calculated from embryos in which the centrosome remained roughly in the middle of the embryo *z*-axis during the recording interval, to simplify the measurement by restricting it to two dimensions. The distance from the centrosome to the nearest point on the embryo cortex (judged as the edge of cytoplasmic GFP) was measured at each time point. Data were smoothed with a running average of five time points. The onset of cortical smoothing was judged from the corresponding DIC images as the first instance of non-ruffling that was propagated away from its initiation site. Establishment of GFP–PAR-2 asymmetry was determined mathematically by comparing maximum intensity values for a 16 pixel × 16 pixel region of the anterior and posterior cortices. A posterior:anterior PAR-2 ratio greater than 1.5 was considered asymmetric. Centrosome–cortex distances behaved similarly in GFP–SPD-2, GFP–PAR-2; GFP–SPD-2 and GFP–SAS-4 embryos (data not shown).

Laser ablations

Laser ablations were performed with the experimental set-up described previously[23], with the following changes. Laser power (before entry into the microscope) was attenuated to less than 5%. About 200 laser pulses at 1,000 MHz were delivered along a 1-μm line through the centrosome. Wide-field GFP images were recorded as described[23].

Centrosome ablations before polarity establishment were performed only in embryos in which the centrosome was at least about 3 μm away from the cortex and roughly in the middle of the *z*-axis of the embryo, to avoid damage to the cortex. Control ablations in pre-polarity embryos were performed by targeting the nucleus (n = 4) or cytoplasm (n = 8) within about 5 μm of the centrosome (and away from the cortex) or the cortex away from the centrosome (n = 7) and ablating the region under the same conditions as for centrosome ablations. Centrosome ablation during polarity establishment necessitated that we ablate the centrosomes within about 2 μm of the cortex; controls for such ablations were therefore performed by targeting a region of the cortex (within about 2 μm of the outermost extent of GFP–PAR-2) away from the position of the centrosomes (about 5 μm) and ablating the region as for centrosome ablations (Supplementary Movie 7).

PAR-2 domain extension

PAR-2 domain sizes, from posterior pole to anterior PAR-2 boundary, were measured as a distance along the long axis of the embryo. The distances were standardized to the length of the embryo (anterior–posterior axis distance) and are expressed as percentages of embryo length; 0% indicates the posterior pole.

PCM and β-tubulin accumulation

The integrated fluorescence intensity of a circle with a radius of three pixels (roughly the size of an early prophase centrosome) was calculated for both the centrosome and a nearby region of cytoplasm (background) at each time point. Times were standardized to the onset of posterior smoothing. The ratio of centrosomal fluorescence to background over time was plotted for a minimum of five individual embryos for each centrosomal marker (Fig. 3a, individual circles) or each RNAi condition (Fig. 4, data not shown); the combined data sets were subjected to a running average (window size 5, lines in Fig. 3a; window size 25, Fig. 4a). In α-tubulin(RNAi), α-/β-tubulin(RNAi) and spd-5(RNAi) embryos there was no evident centrosomal GFP–β-tubulin and we therefore calculated the fluorescence intensity for bright GFP–β-tubulin foci in the region of the male pronucleus.

RNAi

RNAi experiments were performed as described[20]. The primers used for the production of double-stranded RNA *in vitro* are listed in Supplementary Table S1. Worms were grown for 22–25 h (depending on the individual double-stranded RNA) at 25 °C after injection.

PAR-2 tracking

We manually generated kymographs of PAR-2 boundaries from time-lapse images. The *xyt* position of the anterior edge of GFP–PAR-2 was tracked manually. The maximum embryo length (distance from anterior to posterior) from the recording was standardized to 1.0 and all other values are given as fractions of this maximum embryo length. The anterior boundaries of PAR-2 (solid lines) were projected onto the anterior–posterior axis (or the long axis if polarity was not established), displayed as the *x*-axis of the graphs; the cortical PAR-2 domain is indicated by dotted lines. The position of PAR-2 was plotted for each time point, represented along the *y*-axis. Migration of the pronuclei was plotted by using the same process as that described for PAR-2 boundaries; *xyt* positions of the nuclei were determined by the exclusion of cytoplasmic GFP from the images.

Immunofluorescence

Immunofluorescence was performed as described[19] with the use of DM1α (1:100; Sigma) and PAR-2a[24] (1:100) antibodies; these were visualized with fluorescent-conjugated secondary antibodies (Jackson Immunochemicals), and a directly labelled SPD-2 antibody[11] was used to detect centrosomes. Wide-field images were acquired and deconvolved as described[20].

1. Hamill, D. R., Severson, A. F., Carter, J. C. & Bowerman, B. Centrosome maturation and mitotic spindle assembly in *C. elegans* require SPD-5, a protein with multiple coiled-coil domains. *Dev. Cell* **3**, 673–684 (2002).
2. O'Connell, K. F., Maxwell, K. N. & White, J. G. The spd-2 gene is required for polarization of the anteroposterior axis and formation of the sperm asters in the *Caenorhabditis elegans* zygote. *Dev. Biol.* **222**, 55–70 (2000).
3. Goldstein, B. & Hird, S. N. Specification of the anteroposterior axis in *Caenorhabditis elegans*. *Development* **122**, 1467–1474 (1996).
4. Sadler, P. L. & Shakes, D. C. Anucleate *Caenorhabditis elegans* sperm can crawl, fertilize oocytes and direct anterior–posterior polarization of the 1-cell embryo. *Development* **127**, 355–366 (2000).
5. Cuenca, A. A., Schetter, A., Aceto, D., Kemphues, K. & Seydoux, G. Polarization of the *C. elegans* zygote proceeds via distinct establishment and maintenance phases. *Development* **130**, 1255–1265 (2003).
6. Wallenfang, M. R. & Seydoux, G. Polarization of the anterior–posterior axis of *C. elegans* is a microtubule-directed process. *Nature* **408**, 89–92 (2000).
7. Boyd, L., Guo, S., Levitan, D., Stinchcomb, D. T. & Kemphues, K. J. PAR-2 is asymmetrically distributed and promotes association of P granules and PAR-1 with the cortex in *C. elegans* embryos. *Development* **122**, 3075–3084 (1996).
8. Hung, T. J. & Kemphues, K. J. PAR-6 is a conserved PDZ domain-containing protein that colocalizes with PAR-3 in *Caenorhabditis elegans* embryos. *Development* **126**, 127–135 (1999).
9. Etemad-Moghadam, B., Guo, S. & Kemphues, K. Asymmetrically distributed PAR-3 protein contributes to cell polarity and spindle alignment in early *C. elegans* embryos. *Cell* **83**, 743–752 (1995).
10. Guo, S. & Kemphues, K. J. *par-1*, a gene required for establishing polarity in *C. elegans* embryos,

letters to nature

encodes a putative Ser/Thr kinase that is asymmetrically distributed. *Cell* **81**, 611–620 (1995).

11. Pelletier, L. *et al.* The Caenorhabditis elegans centrosomal protein SPD-2 is required for both pericentriolar material recruitment and centriole duplication. *Curr. Biol.* **14**, 863–873 (2004).
12. Hannak, E. *et al.* The kinetically dominant assembly pathway for centrosomal asters in *Caenorhabditis elegans* is gamma-tubulin dependent. *J. Cell Biol.* **157**, 591–602 (2002).
13. Albertson, D. G. Formation of the first cleavage spindle in nematode embryos. *Dev. Biol.* **101**, 61–72 (1984).
14. Strome, S. *et al.* Spindle dynamics and the role of gamma-tubulin in early *Caenorhabditis elegans* embryos. *Mol. Biol. Cell* **12**, 1751–1764 (2001).
15. Kemp, C. A., Kopish, K. R., Zipperlen, P., Ahringer, J. & O'Connell, K. F. Centrosome maturation and duplication in *C. elegans* require the coiled-coil protein SPD-2. *Dev. Cell* **6**, 511–523 (2004).
16. Stevenson, V. A., Kramer, J., Kuhn, J. & Theurkauf, W. E. Centrosomes and the Scrambled protein coordinate microtubule-independent actin reorganization. *Nature Cell Biol.* **3**, 68–75 (2001).
17. Berdnik, D. & Knoblich, J. A. *Drosophila* Aurora-A is required for centrosome maturation and actin-dependent asymmetric protein localization during mitosis. *Curr. Biol.* **12**, 640–647 (2002).
18. Piel, M., Nordberg, J., Euteneuer, U. & Bornens, M. Centrosome-dependent exit of cytokinesis in animal cells. *Science* **291**, 1550–1553 (2001).
19. Gonczy, P. *et al.* Dissection of cell division processes in the one cell stage *Caenorhabditis elegans* embryo by mutational analysis. *J. Cell Biol.* **144**, 927–946 (1999).
20. Oegema, K., Desai, A., Rybina, S., Kirkham, M. & Hyman, A. A. Functional analysis of kinetochore assembly in *Caenorhabditis elegans*. *J. Cell Biol.* **153**, 1209–1226 (2001).
21. Praitis, V., Casey, E., Collar, D. & Austin, J. Creation of low-copy integrated transgenic lines in *Caenorhabditis elegans*. *Genetics* **157**, 1217–1226 (2001).
22. Kirkham, M., Muller-Reichert, T., Oegema, K., Grill, S. & Hyman, A. A. SAS-4 is a *C. elegans* centriolar protein that controls centrosome size. *Cell* **112**, 575–587 (2003).
23. Grill, S. W., Howard, J., Schaffer, E., Stelzer, E. H. & Hyman, A. A. The distribution of active force generators controls mitotic spindle position. *Science* **301**, 518–521 (2003).
24. Pichler, S. *et al.* OOC-3, a novel putative transmembrane protein required for establishment of cortical domains and spindle orientation in the P(1) blastomere of *C. elegans* embryos. *Development* **127**, 2063–2073 (2000).

....

Meiotic catastrophe and retrotransposon reactivation in male germ cells lacking Dnmt3L

Déborah Bourc'his & Timothy H. Bestor

Department of Genetics and Development, College of Physicians and Surgeons of Columbia University, 701 West 168th Street, New York, New York 10032, USA

....

Mammalian genomes employ heritable cytosine methylation in the long-term silencing of retrotransposons and genes subject to genomic imprinting and X chromosome inactivation. Little is known of the mechanisms that direct cytosine methylation to specific sequences. Here we show that DNA methyltransferase 3-like (Dnmt3L (ref. 1)) is expressed in testes during a brief perinatal period in the non-dividing precursors of spermatogonial stem cells at a stage where retrotransposons undergo *de novo* methylation. Deletion of the *Dnmt3L* gene prevented the *de novo* methylation of both long-terminal-repeat (LTR) and non-LTR retrotransposons, which were transcribed at high levels in spermatogonia and spermatocytes. Loss of Dnmt3L from early germ cells also caused meiotic failure in spermatocytes, which do not express Dnmt3L. Whereas dispersed repeated sequences were

demethylated in mutant germ cells, tandem repeats in pericentric regions were methylated normally. This result indicates that the Dnmt3L protein might have a function in the *de novo* methylation of dispersed repeated sequences in a premeiotic genome scanning process that occurs in male germ cells at about the time of birth.

Lifelong gene silencing is imposed on target sequences by *de novo* methylation in germ cells and early embryos. The only factors known to be involved in the establishment of methylation patterns in germ cells are Dnmt3A (ref. 2) and Dnmt3L, a protein that lacks the catalytic motifs that characterize the DNA cytosine-5-methyltransferases but is related to the active DNA methyltransferases Dnmt3A and Dnmt3B in framework regions[1]. Deletion of *Dnmt3L* does not prevent oogenesis, but the heterozygous offspring of homozygous mutant females die before mid-gestation as a result of biallelic expression of imprinted genes normally methylated and silenced on the allele of maternal origin[3]. Male mice that lack Dnmt3L are viable but sterile, with a complete absence of germ cells in adult males[3].

As shown in Fig. 1, expression of Dnmt3L is first seen in non-dividing prospermatogonia after 12.5 days post coitus (d.p.c.) and is highest at about the time of birth; expression declines rapidly after birth and is extinguished by 6 days post partum (d.p.p.), when most prospermatogonia have differentiated into dividing spermatogonial stem cells. Other data show that the decline in Dnmt3L expression over this period is more than 200-fold[4]. Dnmt3L shows striking sexual dimorphism in expression patterns; it is present in females only in growing oocytes, which are arrested in the diplotene stage of meiosis I, but in males it is restricted to diploid prospermatogonia, which differentiate into spermatogonia and undergo many mitotic divisions before entry into meiosis.

The germ cell population of testes lacking Dnmt3L was normal at birth, but only spermatogonia and leptotene and zygotene spermatocytes were seen in testes of young adult males; progressive loss of spermatogonia caused complete azoospermia in older mutant animals. Examination of meiotic chromosome spreads stained with antibodies against synaptonemal complex proteins 1 and 3 (Scp1 and Scp3 (ref. 5)) showed widespread nonhomologous synapsis with branching and anastomosing arrays of synaptonemal complex proteins in most leptotene and zygotene spermatocytes (compare control in Fig. 2a to mutant in Fig. 2b). Some leptotene spermatocytes had complexes of synaptonemal proteins in the form of interlocked rings and other highly abnormal structures (Fig. 2c, d). All spermatocytes showed asynapsis or abnormal synapsis, and none progressed to the full pachytene stage, as assessed by the
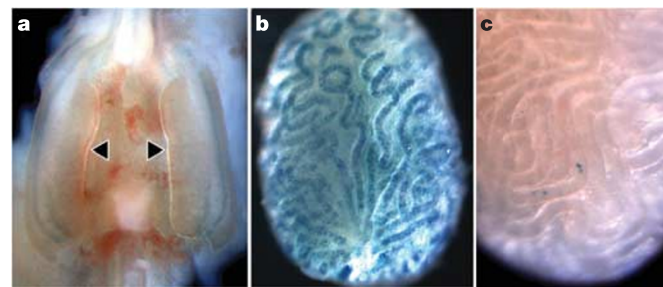

Figure 1 Expression of Dnmt3L in perinatal male germ cells. Dnmt3L transcription was revealed by staining whole testes for β-galactosidase in animals heterozygous for the deletion–*β-geo* insertion allele of *Dnmt3L* described in ref. 3. **a**, Lack of *Dnmt3L* expression in testes (black arrows) at 12.5 d.p.c. **b**, High-level expression of *Dnmt3L* in germ cells at 2 d.p.p.; the β-galactosidase staining visible in the seminiferous tubules was confirmed to be in prospermatogonia by examination of sectioned specimens. **c**, Loss of *Dnmt3L* expression in germ cells in seminiferous tubules of 6 d.p.p. testis.